AIMS Materials Science, 7(3): 302–311.
DOI: 10.3934/matersci.2020.3.302
Received: 04 February 2020
Accepted: 03 June 2020
Published: 05 June 2020

http://www.aimspress.com/journal/Materials

Research article

Rapid facile synthesis of Cu_2ZnSnS_4 films from melt reactions

Mundher Al-Shakban[1,*], Naktal Al-Dulaimi[2,3], Thokozani Xaba[4] and Ahmad Raheel[5]

[1] Department of Physics, College of Science, University of Misan, Maysan, Iraq
[2] Pharmaceutical Chemistry Department, Medical and Applied Science College, Charmo University, 46023 Chamchamal-Sulaimani, Kurdistan Region, Iraq.
[3] Charmo Center for Research and Training, Charmo University, 46023 Chamchamal-Sulaimani, Kurdistan Region, Iraq
[4] Department of Chemistry, Vaal University of Technology, P/Bag X021, Vanderbijlpark, South Africa
[5] Department of Chemistry, Quaid-i-Azam University, Islamabad 45320 Pakistan

* **Correspondence:** Email: mundher.al-shakban@uomisan.edu.iq; Tel: +9647728037980.

Abstract: Films of Cu_2ZnSnS_4 (CZTS) were successfully deposited on glass substrates using blade technique in 5 min annealing time. The effect of heating temperature on the structural properties was investigated. The dithiocarbamates complexes of copper, zinc and tin were used as precursors through the blade technique. The films were kesterite phase and oriented preferentially along (112) direction. The chemical compositions at each temperature were studied in order to optimize the film stoichiometry. Cu/(Zn + Sn) ratio was between 0.815 and 0.877, and Zn/Sn was in the range of 0.93 to 1.

Keywords: single source precursor; dithiocarbamates; blade technique; melt reactions

1. Introduction

Metal xanthates $[M(S_2COR)_x]$ and dithiocarbamates $[M(S_2CNR_2)_x]$, where R is an alkyl group, are excellent precursors to metal sulfides [1–6]. Dithiocarbamates show high thermal stability and their thermal decompositions generally start from 200 °C, which make them suitable to be used as single source precursors for the growth of metal sulfides.

Semiconductor films of Cu_2ZnSnS_4 (CZTS) have high absorption coefficient (10^4 cm^{-1}), and a direct band gap of about 1.5 eV. These factors couple with the fact that CZTS semiconductor consists

of non-toxic and earth abundant elements which makes CZTS an ideal candidate for photovoltaic applications [7]. The photoelectrical performance of CZTS is highly dependent on good stoichiometric control. It is well known that single phase CZTS presents in narrow range of compositions [8], the compositional variation in range of 2–3% can make it difficult to control the structure of the target phase and could lead to phase separation [9–12].

CZTS films have been produced lately using different techniques such as the annealing of Zn/Cu/Sn metals [13] or CuS/SnS/ZnS metal sulfides [14] layers under sulfur atmosphere, flux assisted chemical spray [15], thermal evaporation under vacuum [16,17], sol-gel [18,19], spin coating [20] and chemical vapour deposition [21].

Blade technique (BT) is a perfectly-understood laboratory method that is used to deposit semiliquid precursors (paste) which result in high uniformly thin film. In the former technique, the paste is deposited moderately over the substrates using a coating knife [22]. The quality of the films is dependent on both precursor properties and the blading parameters such as gap width between blade and substrate, annealing temperature, viscosity of the precursor and blading speed. In BT method, the entire precursor is fully used, which makes it a completely material saving method [23,24]. Pure metals and metal acetates have been commonly used as pastes for the deposition of CZTS films by BT method, however CZTS films produced may contain impurities [25] or require long heating time [26]. O'Brien et al. have reported the preparation of $Co_{1-x}S$ [27], ZnS, CdS [28], SnS [29,30], ReS_2 [31], $Mo_{1-x}Re_xS_2$ [32] and FeS_2 [33] from dithiocarbamates complexes by aerosol assisted chemical vapour deposition (AACVD) method.

In this work, a rapid, non-vacuum and without sulfuration process to deposit CZTS films on glass is reported. The method is based on a fast annealing schedule of the paste which contains $[Cu(S_2CNEt_2)_2]$, $[Zn(S_2CNEt_2)_2]$ and $[Sn(C_4H_9)_2(S_2CN(C_2H_5)_2)_2]$ as precursors. We focus on both annealing temperature and the role of the dialkyldithiocarbamates ligand in the decomposition process for their potential in controlling the compositional properties of the CZTS films.

2. Materials and methods

Chemicals purchased from Sigma Aldrich were sodium diethyldithiocarbamate salt, chloroform (99.8%), toluene (99.7%), ethanol (99.8%) and methanol (99.8%). Copper(II) sulfate (98%) was purchased from Fisher chemical while the zinc chloride (98%) was purchased from GPR. All of the chemicals were used without further purification.

2.1. Preparation of bis(diethyldithiocarbamato)copper(II)

$Cu(S_2CNEt_2)_2$ complex was prepared using the reported procedure [34] by the slow addition of methanolic solution of $CuSO_4$ (2.77 g, 0.011 mol) to sodium diethyldithiocarbamate salt (5 g, 0.02219 mol) in methanol (50 mL) with a constant stirring for one hour at room temperature. A black precipitate was obtained, filtered, and washed three times with methanol, and dried in a vacuum oven at room temperature for 10–12 h. Recrystallization was achieved using chloroform. Percentage yield was found to be 2.89 g, 0.008 mol, 73% yield. M.pt. = 192–197 °C. Elemental analysis: calc. for $C_{10}H_{20}CuN_2S_4$ (%): C 33.37, H 5.6, N 7.79, S 35.55. Found (%): C 33.41, H 5.90, N 7.55, S 35.58. The percentage errors for C, H, N and S were 0.12%, 5.35%, 3.08% and 0.08% respectively. FTIR

(cm^{-1}): 2972.2 (w), 2920.2 (w), 1501.8 (s), 1435.2 (s), 1352.3 (w), 1299.7 (s), 1268.4 (s), 1206.7 (s), 1146.9 (s), 1096.8 (m), 1071.7 (s), 996.53 (s), 910.23 (s), 845.15 (s), 778.13 (s) (Figure S1a).

2.2. Preparation of bis(diethyldithiocarbamato)zinc(II)

$Zn(S_2CNEt_2)_2$ complex was prepared using the similar procedure as in 2.1 above using zinc chloride (1.5121 g, 0.011 mol). A white precipitate was obtained and filtered by vacuum filtration. The product was washed three times with methanol and dried in a vacuum oven at 50 °C for 10–12 h to evaporate the remaining solvent. Recrystallization was achieved using chloroform. Percentage yield was found to be 3.2 g, 0.0088 mol, 80.4% yield. M.pt. = 183–187 °C. Elemental analysis: calc. for $C_{10}H_{20}ZnN_2S_4$ (%): C 33.20, H 5.57, N 7.75, S 35.37. Found (%): C 32.93, H 6.40, N 7.72, S 34.97. The percentage errors for C, H, N and S were 0.81%, 14.4%, 0.38% and 1.64%, respectively. FTIR (cm^{-1}): 2968.87 (w), 2930.30 (w), 1499.86 (s), 1427.54 (s), 1377.40 (w), 1353.78 (m), 1297.37 (m), 1270.86 (s), 1200.47 (s), 1144.54 (m), 1096.8 (m), 1072.2 (s), 992.19 (s), 914.10 (s), 839.36 (m), 777.65 (m), 611.80 (w), 562.63 (m) (Figure S1b).

2.3. Synthesis of bis(diethyldithiocarbamato) (di-butyl) tin(IV)

Similar procedure as in 2.1 above was used to prepare $[Sn(C_4H_9)_2(S_2CN(C_2H_5)_2)_2]$ by mixing 50 mL of di-n-butyl tin dichloride (3.37 g, 0.01 mol) in methanol and methanolic solution of sodium diethyldithiocarbamate salt (5 g, 0.022 mol). A white precipitate was obtained which was filtered by vacuum filtration. The product was washed three times with methanol and dried in a vacuum oven at room temperature for one hour. The complex was recrystallized from ethanol and chloroform in ratio 1:2. Percentage yield was found to be 3.7 g, 0.007 mol, 70% yield. M.pt. = 167–172 °C. Elemental analysis: calc. for $C_{18}H_{38}SnN_2S_4$ (%): C 40.86, H 7.24, N 5.29, S 24.17. Found (%): C 39.42, H 7.92, N 4.92, S 22.93. The percentage errors for C, H, N and S were 3.52%, 9.39%, 6.99% and 5.13% respectively. FTIR (cm^{-1}): 2955.8 (w), 2930.70 (w), 1355.20 (m), 1299.78 (m), 1265.07 (s), 1204.8 (s), 1138.27 (s), 1064.51 (s), 1016.30 (m), 993.16 (s), 915.53 (s), 872.14 (s), 839.84 (s), 776.20 (m), 688.56 (s), 568.89 (m) (Figure S1c).

2.4. Preparation of Cu_2ZnSnS_4 films

CZTS films were deposited on glass substrates via the Blade technique. The glass substrates were cleaned with deionized water followed by ultra-sonication for 20 min in acetone. The paste was prepared by mixing $[Cu(S_2CNEt_2)_2]$ (0.005 mmol, 1.798 g), $[Zn(S_2CNEt_2)_2]$ (0.0025 mmol, 0.9 g) and $[Sn(C_4H_9)_2(S_2CN(C_2H_5)_2)_2]$ (0.0025 mmol, 1.32 g) precursors. The mixture was crushed using the mortar and pestle. The paste was ground for about 10 min, and 3 mL of toluene was added with continuous grinding for further two minutes. The mixture was spread using the BT apparatus (Figure 1b) on glass substrates then, the films were loaded into a tube furnace and annealed in nitrogen environment at 375–450 °C for five minutes. The nitrogen flow rate was constant (140 cm^3/min) during the annealing process.

2.5. Characterization techniques

Elemental analysis of complexes was achieved using Flash 2000 TS elemental analyzer. Thermogravimentric Analysis (TGA) was carried out by METTLER TOLEDO TGA/DSC 1 star^{e} system between the ranges of 30–600 °C at a heating rate of 10 °C·min^{-1} under nitrogen atmosphere. FTIR spectra of compounds were recorded on a Specac ATR. Scanning Electron Microscope (SEM) analysis was observed using a Philips XL 30FEG, the molar and atomic ratios were analyzed using a DX4 instrument. Structural characterization of the films was investigated by a Bruker D8 Advance diffractometer with monochromatic Cu-Kα source (λ = 1.5418 Å) at 40 kV and 30 mA, the films were recorded between 20° and 80°.

3. Results and discussion

The IR spectra of $[Cu(S_2CNEt_2)_2]$, $[Zn(S_2CNEt_2)_2]$, and $[Sn(C_4H_9)_2(S_2CN(C_2H_5)_2)_2]$ show bands corresponding to ν(C–S) and ν(C–N) at the ranges between 992–996 and 1499–1501 cm^{-1}, respectively (Figure S1). The thermal decomposition behaviours of $[Cu(S_2CNEt_2)_2]$, $[Zn(S_2CNEt_2)_2]$, and $[Sn(C_4H_9)_2(S_2CN(C_2H_5)_2)_2]$ complexes were studied using thermogravimetric analysis (Figure 1a and Table S1). The major decomposition occurs from 300 to 350 °C. The residual amount of $[Cu(S_2CNEt_2)_2]$ complex found to be about 25.2% which is close to the calculated percentage of CuS (26.56%). Decomposition curve of $[Zn(S_2CNEt_2)_2]$ complex shows a steady mass loss of 94.87% which is starting at about 230 °C and reach a plateau at 360 °C. The first decomposition of $[Sn(C_4H_9)_2(S_2CN(C_2H_5)_2)_2]$ complex begins at 176 °C and finished at 267 °C with a mass loss of 58.969% that correspond to the significant product of the complex. The second decomposition step happened between 268 and 320 °C with the weight loss was of 32.11%. The residues were 4.5% and 9% of the original weight for $[Zn(S_2CNEt_2)_2]$ and $[Sn(C_4H_9)_2(S_2CN(C_2H_5)_2)_2]$ complexes respectively. These values are lower than the theoretical percentage for ZnS (26.94%) and SnS (28.49%). Weight losses take place due to sublimation occurs during the TGA analysis [34,30,35].

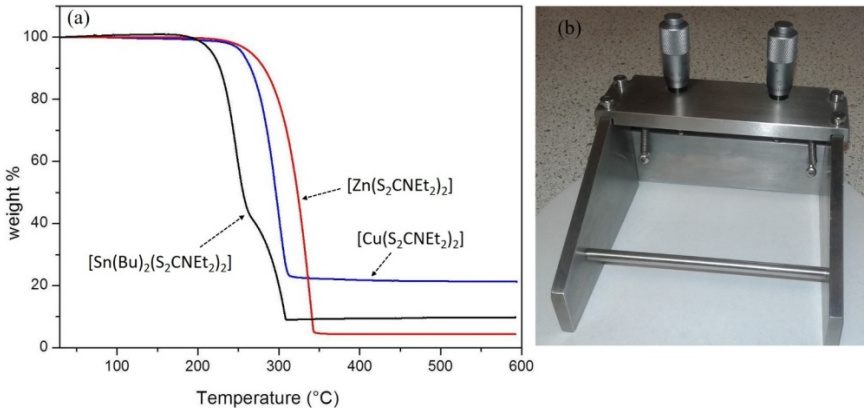

Figure 1. (a) Thermal analysis curves of $[Cu(S_2CNEt_2)_2]$, $[Zn(S_2CNEt_2)_2]$ and $[Sn(C_4H_9)_2(S_2CN(C_2H_5)_2)_2]$ complexes and (b) blade coater.

The kesterite phase of CZTS was successfully deposited by the blade technique. All of the diffraction peaks in Figure 2 can be indexed to tetragonal phase of CZTS (JCPDS no 26-0575). The

patterns show well-defined peaks that are assigned to (112), (220) and (312) planes of CZTS tetragonal structure. The (112) plane is a preferred orientation of CZTS films.

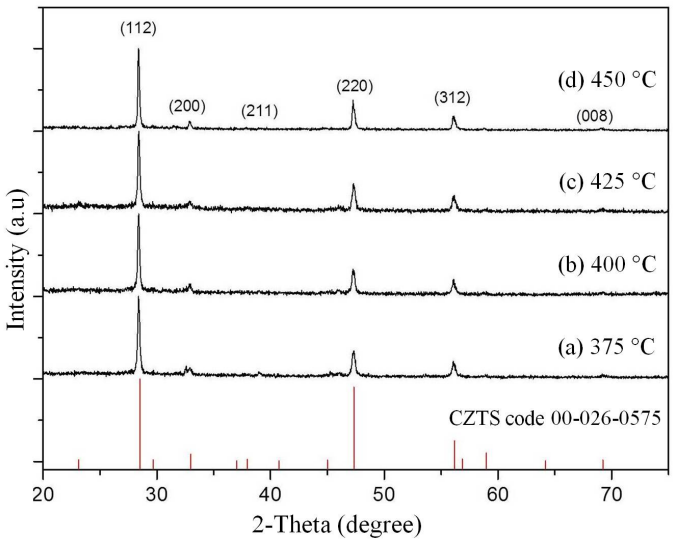

Figure 2. The powder X-ray diffraction (p-XRD) patterns of CZTS films deposited by blade technique (BT) from $[Cu(S_2CNEt_2)_2]$, $[Zn(S_2CNEt_2)_2]$, and $[Sn(C_4H_9)_2(S_2CN(C_2H_5)_2)_2]$ precursors.

The degree of preferred orientation of the (112), (220) and (321) planes were found through measuring texture coefficient (T_C) using the literature method [14,36]. The estimated T_C values are presented in Table S2 and Figure 3. The values of T_C at (112) and (321) showed a slight variation compared to the (220). The (112) crystalline phase reveals higher T_C = 1.42–1.53 than that of other phases. The higher values of T_C correspond to the increase in planar density along (112) plane [37]. The present study shows that the use of dialkyldithiocarbamates can achieve highly oriented (112) crystalline plane through blade technique under atmospheric pressure and without sulfuration.

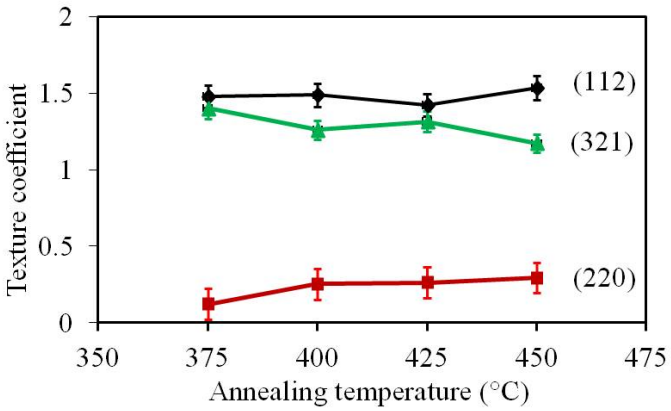

Figure 3. Texture coefficient of CZTS films prepared at 375, 400, 425 and 450 °C from $[Cu(S_2CNEt_2)_2]$, $[Zn(S_2CNEt_2)_2]$, and $[Sn(C_4H_9)_2(S_2CN(C_2H_5)_2)_2]$ precursors.

Raman spectrum of a CZTS film heated at 375 °C is reported in Figure S2. The spectrum showed that the dominant peak is located at 335 cm^{-1}. This peak corresponds to A vibration mode of CZTS [38–40]. There were no signals of secondary phases such as ZnS, Cu_2SnS_3 and $Cu_{2-x}S$ that were found. It was noted that the Raman peak was below 337 cm^{-1}, which is the strongest peak assigned as A mode of kesterite CZTS. In kesterite planes, when the ratio of Cu/(Zn + Sn) is less than one (Table S2), the concentration of defects becomes larger. The random distribution of defects appeared when Cu substitutes for Zn at the 2*d* site and/or Zn substitute Cu at the 2*c* site [41,42]. In this case, the disordered kesterite CZTS will be effective. The disordered kesterite structure is similar to stannite CZTS. Therefore, we propose that the shift toward the low wave number direction can be attributed to the disordered kesterite CZTS [43,44].

Figure 4 shows SEM images of CZTS films annealed at 375, 400, 425 and 450 °C on a glass substrate. The films were found to be between 1.9 and 3.4 μm thick, Grain growth occurs for the films heated at 400 and 425 °C for 5 min and the sizes of the grains were more than 1 μm. When the temperature was increased to 450 °C, the cube like shape particles were observed with grain size up to 0.5 μm.

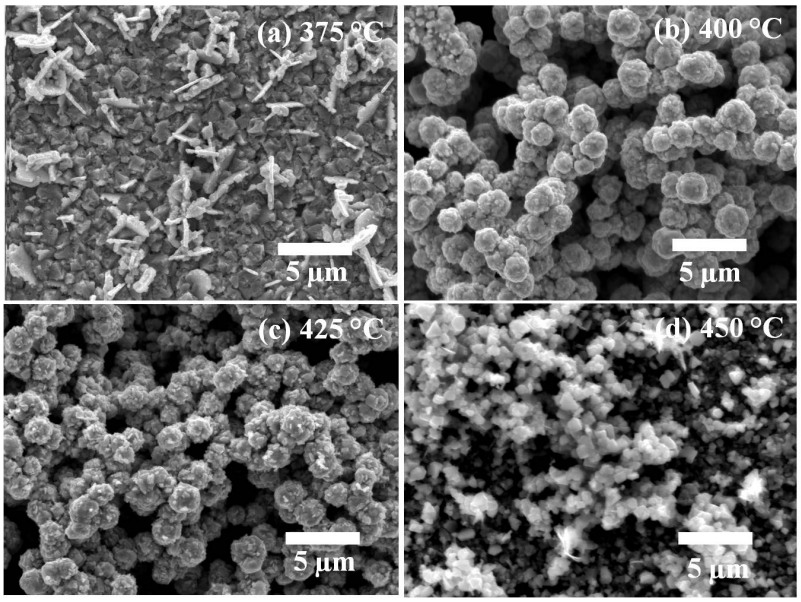

Figure 4. SEM micrograms of CZTS films deposited by blade technique annealed at (a) 375 °C, (b) 400 °C, (c) 425 °C, and (d) 450 °C.

The EDS analysis shows the elemental stoichiometry of the CZTS films. The concentrations of dialkyldithiocarbamate precursors that have been given in the experimental section obtained films with 2:1:1:4 elemental ratios of Cu:Zn:Sn:S. The elemental compositions are presented in Figure 5a and Table S3. The Cu/(Zn + Sn) and the Zn/Sn ratios changed due to the annealing temperature. The CZTS films that were heated at 375, 400, 425 and 450 °C revealed poor Cu residue and rich with Zn content (Figure 5b). The results also show that there is slight varation in the value of copper with increased the temperature, as well as Cu/(Zn + Sn) and Zn/Sn ratios of 0.877 and 1 was found to be larger at 375 ^{o}C. The S/(Cu + Zn + Sn) ratio, however, does not show a clear dependence on the

anealing tempretures. This information suggests that there is no major sulfur loss in films as the temperture is raised.

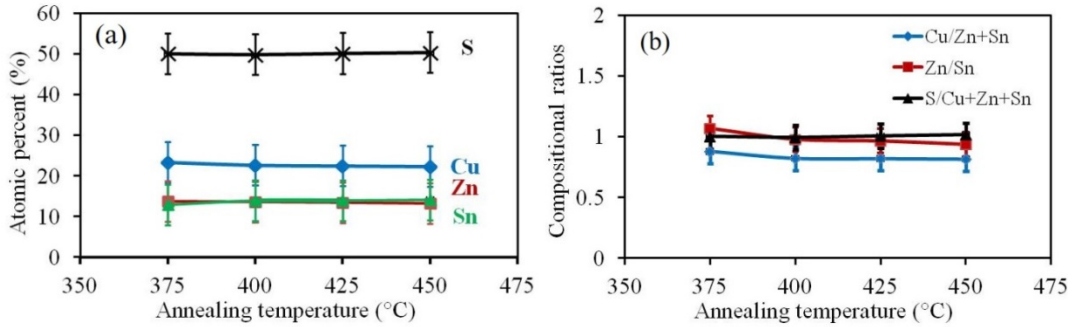

Figure 5. (a) Elemental compositions and (b) compositional ratios of CZTS films determined by energy-dispersive X-ray spectroscopy.

4. Conclusions

The decompositions of a series of N,N-dialkyldithiocarbamates complexes of copper, zinc and tin were investigated by thermogravimetric analysis. The combination of $[Cu(S_2CNEt_2)_2]$, $[Zn(S_2CNEt_2)_2]$, and $[Sn(C_4H_9)_2(S_2CN(C_2H_5)_2)_2]$ precursors was used as a paste for the formation of Cu_2ZnSnS_4 through doctor blade technique. The p-XRD patterns of the prepared CZTS films that were obtained after heating at temperatures between 375 and 450 ^oC confirmed tetragonal phase structure. The EDS measurements show that the Cu/(Zn + Sn) ratio was between 0.815 and 0.877. The heating of dialkyldithiocarbamates complexes to high temperatures for short periods of time gives kesterite phase CZTS which may be suitable for photovoltaic applications.

Acknowledgements

The authors would like to acknowledge the support that is given by Iraqi Culture Attache´ in London and Ministry of higher education and scientific research in Iraq for financial support. The authors would also like to thank Prof. Paul O'Brien and Dr. David Lewis at School of Materials University of Manchester for their contribution.

Conflict of interests

All authors declare no conflicts of interest in this paper.

References

1. Abutbul R, Segev E, Zeiri L, et al. (2016) Synthesis and properties of nanocrystalline π-SnS—a new cubic phase of tin sulphide. *RSC Adv* 7: 5848–5855.
2. Rabkin A, Samuha S, Abutbul R, et al. (2015) New nanocrystalline materials: a previously unknown simple cubic phase in the SnS binary system. *Nano lett* 15: 2174–2179.

3. Al-Shakban M, Matthews P, O'Brien P (2017) A simple route to complex materials: the synthesis of alkaline earth-transition metal sulfides. *Chem Commun* 53: 10058–10061.
4. Alqahtani T, Khan M, Kelly D, et al. (2018) Synthesis of $Bi_{2-2x}Sb_{2x}S_3$ ($0 \leq x \leq 1$) solid solutions from solventless thermolysis of metal xanthate precursors. *J Mater Chem C* 6: 12652–12659.
5. Al-Shakban M, Matthews P, Lewis E, et al. (2019) Chemical vapor deposition of tin sulfide from diorganotin (IV) dixanthates. *J Mater Sci* 54: 2315–2323.
6. Al-Shakban M, Matthews P, et al. (2018) On the phase control of $CuInS_2$ nanoparticles from Cu-/In-xanthates. *Dalton T* 47: 5304–5309.
7. Khalate S, Kate R, Deokate R (2018) A review on energy economics and the recent research and development in energy and the Cu_2ZnSnS_4 (CZTS) solar cells: A focus towards efficiency. *Sol Energy* 169: 616–633.
8. Du H, Yan F, Young Y, et al. (2014) Investigation of combinatorial coevaporated thin film Cu_2ZnSnS_4. I. Temperature effect, crystalline phases, morphology, and photoluminescence. *J Appl Phys* 115: 173502.
9. Olekseyuk I, Dudchak I, Piskach L (2004) Phase equilibria in the Cu_2S–ZnS–SnS_2 system. *J Alloy Compd* 368: 135–143.
10. Muska K, Kauk M, Altosaar M, et al. (2011) Synthesis of Cu_2ZnSnS_4 monograin powders with different compositions. *Energy Procedia* 10: 203–207.
11. Jiang C, Liu W, Talapin D (2014) Role of precursor reactivity in crystallization of solution-processed semiconductors: the case of Cu_2ZnSnS_4. *Chem Mater* 26: 4038–4043.
12. Zutz F, Chory C, Knipper M, et al. (2015) Synthesis of Cu_2ZnSnS_4 nanoparticles and analysis of secondary phases in powder pellets. *Phys Status Solidi A* 212: 329–335.
13. Alvarez A, Exarhos S, Mangolini L (2016) Tin disulfide segregation on CZTS films sulfurized at high pressure. *Mater Lett* 165: 41–44.
14. Sánchez T, Mathew X, Mathews N (2016) Obtaining phase-pure CZTS thin films by annealing vacuum evaporated CuS/SnS/ZnS stack. *J Cryst Growth* 445: 15–23.
15. Thankalekshmi R, Sidhu N, Rastogi A (2017) Non-Vacuum single step synthesis of large-grain size CZTS photo absorber for thin film solar cells by flux assisted chemical spray. *IEEE 44th PVSC* 3279–3284.
16. Shin B, Gunawan O, Zhu Y, et al. (2013) Thin film solar cell with 8.4% power conversion efficiency using an earth-abundant Cu_2ZnSnS_4 absorber. *Prog Photovoltaics* 21: 72–76.
17. Chalapathi U, Uthanna S, Sundara V (2013) Growth and characterization of co-evaporated Cu_2ZnSnS_4 thin films. *J Renew Sustain Energ* 5: 031610.
18. Park H, Hwang Y, Bae B (2013) Sol-gel processed Cu_2ZnSnS_4 thin films for a photovoltaic absorber layer without sulfurization. *J Sol-Gel Sci Techn* 65: 23–27.
19. Zhang K, Su Z, Zhao L, et al. (2014) Improving the conversion efficiency of Cu_2ZnSnS_4 solar cell by low pressure sulfurization. *Appl Phys Lett* 104: 141101.
20. Al-Shakban M, Matthews M, Savjani N, et al. (2017) The synthesis and characterization of Cu_2ZnSnS_4 thin films from melt reactions using xanthate precursors. *J Mater Sci* 52: 12761–12771.
21. Ramasamy K., Malik M, O'Brien P (2011) The chemical vapor deposition of Cu_2ZnSnS_4 thin films. *Chem Sci* 2: 1170–1172.
22. Ahmadi S, Asim N, Alghoul N, et al. (2014) The role of physical techniques on the preparation of photoanodes for dye sensitized solar cells. *Int J Photoenergy* 2014: 198734.

23. Padinger F, Brabec C, Fromherz T, et al. (2000) Fabrication of large area photovoltaic devices containing various blends of polymer and fullerene derivatives by using the doctor blade technique. *Opto-Electron Rev* 8: 280–283.
24. Kontos A, Kontos A, Tsoukleris D, et al. (2008) Nanostructured TiO_2 films for DSSCS prepared by combining doctor-blade and sol-gel techniques. *J Mater Process Tech* 196: 243–248.
25. Pani B, Singh P (2013) Preparation of Cu_2ZnSnS_4 thin film by a simple and cost effective route using metallic precursors and effect of selenization on these films. *J Renew Sustain Ener* 5: 053131.
26. Mokurala K, Mallick S, Bhargava P (2014) Low temperature synthesis and characterization of Cu2ZnSnS4 (CZTS) nanoparticle by solution based solid state reaction method. *Energy Procedia* 57: 73–78.
27. Ramasamy K, Malik M, Raftery J, et al. (2010) Selective deposition of cobalt sulfide nanostructured thin films from single-source precursors. *Chem Mater* 22: 4919–4930.
28. Ramasamy K, Malik M, Helliwell M, et al. (2011) Thio-and dithio-biuret precursors for zinc sulfide, cadmium sulfide, and zinc cadmium sulfide thin films. *Chem Mater* 23: 1471–1481.
29. Ramasamy K, Kuznetsov V, Gopal K, et al. (2013) Organotin dithiocarbamates: single-source precursors for tin sulfide thin films by aerosol-assisted chemical vapor deposition (AACVD). *Chem Mater* 25: 266–276.
30. Kevin P, Lewis D, Raftery J, et al. (2015) Thin films of tin (II) sulphide (SnS) by aerosol-assisted chemical vapour deposition (AACVD) using tin (II) dithiocarbamates as single-source precursors. *J Cryst Growth* 415: 93–99.
31. Al-Dulaimi N, Lewis D, Zhong X, et al. (2016) Chemical vapour deposition of rhenium disulfide and rhenium-doped molybdenum disulfide thin films using single-source precursors. *J Mater Chem C* 4: 2312–2318.
32. Al-Dulaimi N, Lewis D, Savjani N, et al. (2017) The influence of precursor on rhenium incorporation into re-doped MoS_2($Mo_{1-x}Re_xS_2$) thin films by aerosol-assisted chemical vapour deposition (AACVD). *J Mater Chem C* 5: 9044–9052.
33. O'Brien P, Otway D, Park J (1999) Iron sulfide (FeS_2) thin films from single-source precursors by aerosol-assisted chemical vapor deposition (AACVD). *MRS OPL* 606.
34. Kevin P, Malik M, O'Brien P (2015) The controlled deposition of $Cu_2(Zn_yFe_{1-y})SnS_4$, $Cu_2(Zn_yFe_{1-y})SnSe_4$ and $Cu_2(Zn_yFe_{1-y})Sn(S_xSe_{1-x})4$ thin films by AACVD: potential solar cell materials based on earth abundant elements. *J Mater Chem C* 3: 5733–5741.
35. Khalid S, Ahmed E, Malik M, et al. (2015) Synthesis of pyrite thin films and transition metal doped pyrite thin films by aerosol-assisted chemical vapour deposition. *New J Chem* 39: 1013–1021.
36. Kirubakaran D, Dhas C, Jain S, et al. (2019) Jet nebulizer-spray coated CZTS film as Pt-free electrocatalyst in photoelectrocatalytic fuel cells. *Appl Surf Sci* 463: 994–1000.
37. Kumar M, Kumar A, Abhyankar A (2015) Influence of texture coefficient on surface morphology and sensing properties of w-doped nanocrystalline tin oxide thin films. *ACS Appl Mater Inter* 7: 3571–3580.
38. Seboui Z, Cuminal Z, Kamoun N (2013) Physical properties of Cu_2ZnSnS_4 thin films deposited by spray pyrolysis technique. *J Renew Sustain Ener* 5: 023113.
39. Muhunthan N, Singh O, Singh S, et al. (2013) Growth of CZTS thin films by cosputtering of metal targets and sulfurization in H_2S. *Int J Photoenergy* 2013.

40. Ahmad R, Distaso M, Azimi H, et al. (2013) Facile synthesis and post-processing of eco-friendly, highly conductive copper zinc tin sulphide nanoparticles. *J Nanopart Res* 15: 1886.
41. Washio T, Nozaki H, Fukano T, et al. (2011) Analysis of lattice site occupancy in kesterite structure of Cu_2ZnSnS_4 films using synchrotron radiation X-ray diffraction. *J Appl Phys* 110: 074511.
42. Walsh A, Chen S, Wei S, et al. (2012) Kesterite thin-film solar cells: Advances in materials modelling of Cu_2ZnSnS_4. *Adv Energy Mater* 2: 400–409.
43. Valakh M, Dzhagan V, Babichuk I, et al. (2013) Optically induced structural transformation in disordered kesterite Cu_2ZnSnS_4. *JETP lett* 98: 255–258.
44. Grossberg M, Krustok J, Raudoja J, et al. (2012) The role of structural properties on deep defect states in Cu_2ZnSnS_4 studied by photoluminescence spectroscopy. *Appl Phys Lett* 101: 102102.

AIMS Press